Joint Bidding and Geographical Load Balancing for Datacenters: Is Uncertainty a Blessing or a Curse?

Ying Zhang, Lei Deng, Minghua Chen, and Peijian Wang

***Abstract*—We consider the scenario where a cloud service provider (CSP) operates multiple geo-distributed datacenters to provide Internet-scale service. Our objective is to minimize the total electricity and bandwidth cost by jointly optimizing electricity procurement from wholesale markets and geographical load balancing (GLB), *i.e.*, dynamically routing workloads to locations with cheaper electricity. Under the ideal setting where exact values of market prices and workloads are given, this problem reduces to a simple LP and is easy to solve. However, under the realistic setting where only distributions of these variables are available, the problem unfolds into a non-convex infinite-dimensional one and is challenging to solve. Our main contribution is to develop an algorithm that is proven to solve the challenging problem optimally and efficiently, by exploring the full design space of strategic bidding. Trace-driven evaluations corroborate our theoretical results, demonstrate fast convergence of our algorithm, and show that it can reduce the cost for the CSP by up to 20% as compared to baseline alternatives. Our study highlights the intriguing role of uncertainty in workloads and market prices, measured by their variances. While uncertainty in workloads deteriorates the cost-saving performance of joint electricity procurement and GLB, counter-intuitively, uncertainty in market prices can be exploited to achieve a cost reduction even *larger* than the setting without price uncertainty.**

I. Introduction

As cloud computing services become prevalent, the electricity cost of worldwide datacenters hosting these services has skyrocketed, reaching \$16B in 2010 [20]. Electricity cost represents a large fraction of the datacenter operating expense [36], and it is increasing at an alarming rate of 12% annually [4]. Consequently, reducing electricity cost has become a critical concern for datacenter operators [28].

There have been substantial research on reducing power consumption and related cost of datacenters [15], [17], [33], [35]. Among them, geographical load balancing (GLB) is a promising technique [28], [29], [32]. By *dynamically* routing workloads to locations with cheaper electricity, GLB has been shown to be effective in reducing electricity cost (*e.g.*, by 2–13% [28]) of geo-distributed datacenters operated by a CSP. Many existing works explore price *diversity across geographical locations* to reduce electricity cost [28], [29], [38]. Some recent studies also advocate additional price *diversity across time* at a location, by for example using electricity storage system and demand response for arbitrage [33] or opportunistically optimizing various electricity procurement options [7], [14], [37].

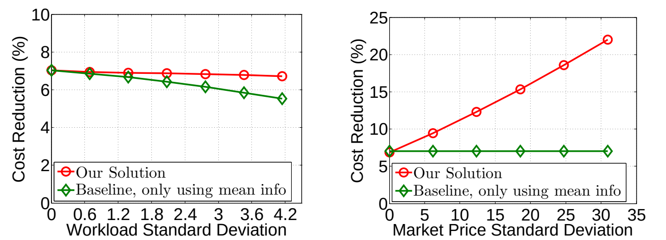

(a) (b)

Fig. 1. (a) We fix market prices to their means and increase standard deviations of workloads. Cost reductions of our solution and baseline decrease as the standard deviations increase. (b) We fix workloads to their means and increase standard deviations of prices. Cost reduction of our solution increases as the standard deviations increase, while that of baseline stays constant. More details are in Sec. V and Sec.VII-C.

Inspired by these advances and recent practices that CSPs moving into electricity markets (*e.g.*, Google Energy LLC [16]), we consider the scenario where a CSP jointly performing GLB and electricity procurement from deregulated markets. The market prices are set by running *auction* mechanisms among the electricity suppliers and consumers, cf, [40]. The goal is to minimize the total electricity and bandwidth cost, by exploiting price diversity in both geographical locations (by GLB) and time (by procurement in local sequential markets).

Under the ideal setting where exact values of market prices and workloads are given, the problem reduces to a simple LP and is easy to solve, by for example the solution in [28]. In practice, however, the actual values of these variables are revealed only at the operating time, and only their distributions are available when procuring electricity by submitting bids to markets (bidding). Under such realistic settings, the problem unfolds into a non-convex infinite-dimensional one. Our focus in this paper is to develop an algorithm to solve the problem optimally.

Our study highlights the intriguing role of uncertainty in workloads and market prices, measured by their variances. On one hand, workload uncertainty undermines the efficiency of balancing supply and demand (proportional to workload) on electricity markets. As a result, the cost-saving performance of joint bidding and GLB deteriorates as workload uncertainty increases, as illustrated in Fig. 1(a). On the other hand, counter-intuitively, higher uncertainty in market prices allows us to extract larger *coordination* gain in sequential procurement in day-ahead and real-time markets [3], [13], [23]. As shown in Fig. 1(b), capitalizing such gain leads to a cost reduction even

Ying Zhang, Lei Deng and Minghua Chen are with Department of Information Engineering, the Chinese University of Hong Kong, Hong Kong. Peijian Wang is with School of Electrical and Information Engineering, Xi'an Jiaotong University, Xi'an, China.

Some results in this paper have been published in its conference version [42].

larger than the setting without price uncertainty.

In our solution, we explore the full design space of strategic bidding to *simultaneously* exploit the price uncertainty and combat the workload uncertainty, so as to maximize the cost saving. We make the following contributions.

▷ We present necessary backgrounds on electricity markets in Sec. II. Then in Sec. III, we formulate the problem of cost minimization by joint bidding and GLB, under the realistic setting where only distributions of market prices and workloads are available. The problem is a non-convex infinite-dimensional one and is in general challenging to solve.

▷ To address the non-convexity challenge, in Sec. IV, we leverage problem structures to characterize a subregion of the feasible set so that (i) it contains the optimal solution, and (ii) the problem over this subregion becomes a convex one. We then solve the reduced problem by a nested-loop solution.

▷ In the inner loop, we fix the GLB decision and optimize bidding strategies for local sequential markets. We derive an easy-to-compute closed-form optimal solution in Sec. IV-B. The optimal bidding strategies not only address the infinite-dimension challenge, but also allow the CSP to simultaneously exploit price uncertainty and combat workload uncertainty.

▷ In the outer loop, we solve the remaining GLB problem given optimal bidding strategies. While the problem is convex and of finite dimension, its objective function does not admit an explicit-form expression. Consequently, its gradient cannot be computed explicitly, and gradient/subgradient-based algorithms cannot be directly applied. In Sec. IV-C, we tackle this issue by adapting a zero-order optimization algorithm, named General Pattern Search (GPS) [21], to solve the problem without knowing the explicit-form expression of the objective function. Finally, we prove that our nested-loop algorithm solves the joint bidding and GLB problem optimally. We discuss the computational complexity and issues related to practical implementation in Sec. IV-D.

▷ We analyze the impact of demand and price uncertainties on the cost-saving performance in Sec. V. Realizing our optimal bidding curve may require CSP to place an infinite number of bids in each deregulated electricity market. In practice, however, market operator may only accept a finite number of bids from the CSP. In Sec. VI, we carefully quantize the optimal bidding curve so that it can be realized by using a finite number of bids. We bound the performance loss due to such quantization.

▷ By evaluations based on real-world traces in Sec. VII, we show that our solution converges fast and reduces the CSP cost by up to 20% as compared to baseline alternatives.

Our study also adds understanding to energy cost management for entities other than datacenters. For example, [27] and [23] considered similar problems for utilities and microgrids, without fully exploring the bidding design space or pursing optimal solution. Results of our study thus can help to optimize bidding strategy designs under such settings.

We discuss related works in Sec. VIII and conclude the paper in Sec. IX. Due to space limitation, some proofs are deferred in our technical report [41].

II. Electricity Market Preliminary

In a region, there are two electricity wholesale markets, *day-ahead* market and *real-time* market, to balance the electricity supply and demand in two timescales. We show the critical operations in Fig. 2 and explain the details in the following.

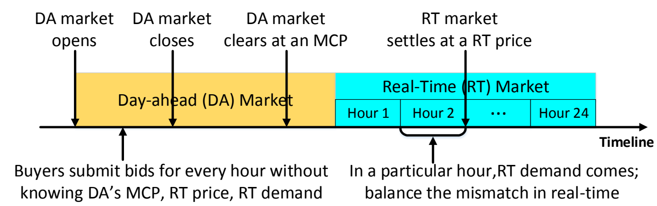

Fig. 2. Operation of day-ahead market and real-time market.

Day-Ahead Market. The day-ahead market is a forward market to trade the electricity one day before dispatching. The electricity supply is auctioned in the day-ahead market. The sellers, *i.e.*, generation companies, submit (hourly) generation offers, and the buyers, *i.e.*, utilities or CSPs, submit (hourly) demand bids, all in the format of <*marginal price, quantity*>, to the *auctioneer*, *i.e.*, the Independent System Operator (ISO).

In the offers (resp. bids), the generation companies (resp. utilities and CSPs) specify the amount of electricity they want to sell (resp. buy) and at which marginal price. Each seller (resp. buyer) is allowed to submit *multiple* offers (resp. bids) [3] in the same auction with different prices and quantities. The ISO matches the offers with the bids, typically using a well-established double auction mechanism [40]. The outcome of the auction is that it determines a *market clearing price* (MCP) for all the traded units. The bids with prices higher than MCP and the offers with prices lower than MCP will be accepted, and the electricity will be traded at MCP. Upon day-ahead market settlement, the generation companies (resp. utilities and CSPs) will be notified the quantity and MCP of electricity that they commit to generate (resp. consume).

The actual value of MCP is revealed only after the day-ahead market is settled/cleared, and they are unknown to market participants at the time of submitting bids/offers.

We show an example in Fig. 3 from the perspective of our CSP. Suppose that the CSP submits three bids to the day-ahead market: <30$/MWh, 3MWh>, <51$/MWh, 4MWh>, <70$/MWh, 5MWh>. Now if ISO announces that the MCP is 40$/MWh after the auction, then the second and the third bid will be accepted since their bidding prices are higher than MCP. Thus the CSP gets $4+5=9$MWh of day-ahead committed supply at the price of MCP, *i.e.*, 40$/MWh. The day-ahead trading cost is thus $9\times 40=360$$.

Real-Time Market. The mismatch between day-ahead committed supply (as discussed above) and real-time demand is balanced on the real-time market, in a pay-as-you-go fashion. In particular, the system calls the short-start fast-responding generating units, which is usually more expensive, to standby and meet the instantaneous power shortage if any. The real-time price is set after the real-time dispatching and are not exactly known a priori.

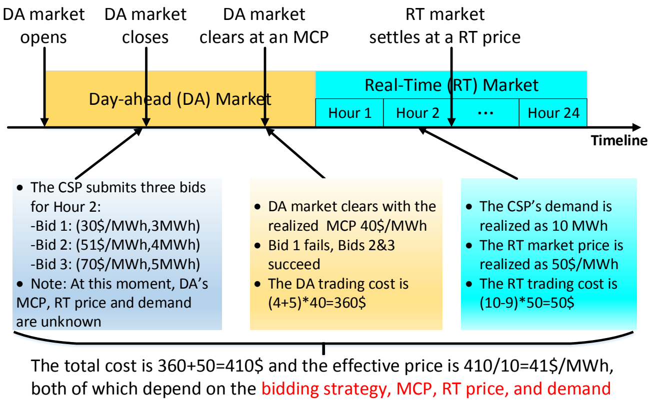

Fig. 3. An illustrating example for the CSP to participate in markets.

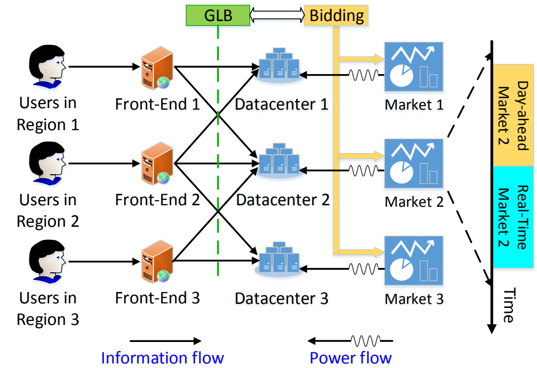

Fig. 4. The scenario that we consider in this paper.

- In case that the day-ahead committed supply matches exactly the actual demand, there is no real-time cost.
- In case of under-supply, (*i.e.*, the committed supply is less than the real-time demand), the CSP will pay for extra supply at the real-time price.
- In case of over-supply, the system needs to reduce the power generation output or pay to schedule elastic load [25] to balance the supply, both incurring operational overhead and consequently economic loss. In this case, the CSP will receive a rebate at price $\beta \cdot$ MCP for the unused electricity (recall that the planned supply is purchased from the day-ahead market at price MCP). Here $\beta \in [0, 1)$ is a discounting factor capturing the overhead-induced cost in handling over-supply situation.

The overall electricity cost for the CSP is the sum of day-ahead procurement cost and the real-time settlement cost, which can be in the form of extra payment or rebate. This pricing model can be viewed as a generalization of the classic Newsvendor problem in operations research [19], and a real-world market example fitting this model can be found in [18]. We remark that the framework developed in this paper can also be extended to different pricing models described in [13], [25], [27] (see our discussions in [41]).

Back to our example for the CSP in Fig. 3, suppose that the CSP's real-time demand is 10MWh. Since the day-ahead committed supply is only 9MWh, *i.e.*, the under-supply case happens, the CSP needs to buy 1MWh extra electricity from the real-time market. Now if the real time price is 50$/MWh, the real-time trading cost of the CSP will be $1 \times 50 = 50$\$. The total cost is the sum of day-ahead trading cost and real-time trading cost, which is 360+50=410$.

Cost Structure. An important observation is that the overall cost depends on not only the actual demand, the day-ahead MCP and the real-time price, but also the mismatch between the day-ahead committed supply and the actual demand. As the day-ahead committed supply depends on day-ahead market bidding strategy of the CSP, the overall cost is thus also a function of the bidding strategy. We remark that such cost structure is unique to electricity procurement in electricity markets and motivates the bidding strategy design [27].

III. System Model and Problem Formulation

We consider the scenario of a CSP providing computing-intensive services (*e.g.*, Internet search) to users in N regions by operating N geo-distributed datacenters, one in each region, as exemplified in Fig. 4. Service workloads from a region can be served either by the local datacenter or possibly by datacenters in other regions through GLB. The CSP directly participates in wholesale electricity markets in each region, to obtain electricity to serve the local datacenter. Based on (i) distributions of hourly service workloads and (ii) distributions of market settlement prices, the CSP aims at minimizing the expected total operating cost by optimizing GLB and bidding strategies in the markets. The hourly timescale aligns with both the settlement timescale in wholesale markets [32] and the suggested time granularity for performing GLB [28].

Without loss of generality, we focus on minimizing cost of a particular operation hour of the CSP, as shown in Fig. 3.

A. Workload and Geographical Load Balancing

Workload and Electricity Demand. We assume that each datacenter is power-proportional, which means that its electricity consumption is proportional to its workload [28]. For example, Google reports that each search requires about 0.28Wh electricity for its datacenters [28]. Without loss of generality, we assume that the workload-to-electricity coefficients are one for all datacenters and thus use the workload served by a datacenter to represent its electricity demand. Our results can be easily generalized to the case where the coefficients are different for different datacenters.

We model the workload originated from region i as a random variable U_i in the range $[\underline{u}_i, \bar{u}_i]$, with a probability density function (PDF) $f_{U_i}(u)$ that can be empirically estimated from historical data. We assume that all U_i's are independent.

Geographical Load Balancing.[1] We denote the GLB deci-

[1]Under the conventional setting where datacenters obtain electricity from utilities, GLB is performed in CSP's real-time operation. Under the setting we consider in this paper, CSP needs to bid for electricity in the day-ahead market, where the amount of electricity to bid is a function of GLB decisions. As such, we consider doing joint GLB and electricity bidding in CSP's day-ahead operation, in order to fully explore the new design space enabled by the setting considered in this paper. It is conceivable to perform GLB in both day-ahead and real-time operations of CSP to further minimize the energy cost, which we leave for future study.

sion by $\boldsymbol{\alpha} = [\alpha_{ij} : i, j = 1, \ldots, N] \in \mathbb{R}_{N \times N}$ which satisfies

$$\sum_j \alpha_{ij} \geq 1, \quad \forall i = 1, \ldots, N, \tag{1}$$

$$\alpha_{ii} \geq \lambda_i, \ \ \forall i = 1, \ldots, N, \tag{2}$$

$$\bar{v}_j \triangleq \sum_{i=1}^{N} \alpha_{ij} \bar{u}_i \leq C_j, \quad \forall j = 1, \ldots, N. \tag{3}$$

$$0 \leq \alpha_{ij} \leq 1, \quad \forall i, j = 1, \ldots, N, \tag{4}$$

$$\alpha_{ij} = 0, \quad \forall (i, j) \in \mathcal{G}, \tag{5}$$

where $\mathcal{G} \triangleq \{(i, j) |$ workloads from region i cannot be routed to datacenter $j\}$ captures the topological constraints.

Here α_{ij} represents the fraction of the workload originated from region i that will be routed to datacenter j. Constraints in (1) mean that all workloads must be served. Constraints in (2) capture that λ_i fraction of the workload originated from region i can only be served locally due to various reasons such as delay requirements. Constraints in (3) ensure that the total workload coming into datacenter j can be served even in the largest realization of workload. Constraints in (5) describe that the workload cannot be routed to a datacenter that is too far away from its own region. We define the set of all feasible GLB decisions as

$$\mathcal{A} \triangleq \{\boldsymbol{\alpha} \in \mathbb{R}^{N \times N} | \boldsymbol{\alpha} \text{ satisfies } (1) - (5)\}. \tag{6}$$

Given the GLB decision $\boldsymbol{\alpha}$, the total workload for datacenter j is given by $V_j = \sum_i \alpha_{ij} U_i$. Since $U_i, \forall i$ are random variables, V_j is also a random variable with a PDF

$$f_{V_j}(v) = f_{U_{1j}} \otimes f_{U_{2j}} \otimes \ldots \otimes f_{U_{Nj}}(v), \tag{7}$$

where $\otimes$ is the convolution operator and the distribution functions in the convolution are given by

$$f_{U_{ij}}(u) = \begin{cases} \frac{1}{\alpha_{ij}} f_{U_i}\left(\frac{u}{\alpha_{ij}}\right), & \text{if } \alpha_{ij} > 0, \\ \delta(u), & \text{if } \alpha_{ij} = 0, \end{cases} \tag{8}$$

where $\delta(\cdot)$ denotes Dirac delta function.

Bandwidth Cost. Let $z_{ij} \geq 0$ be the unit bandwidth cost from region i to datacenter j. The expected network cost of routing the workload to different datacenters is given by

$$\mathsf{BCost}(\boldsymbol{\alpha}) = \sum_{i=1}^{N} \sum_{j=1}^{N} z_{ij} \cdot \alpha_{ij} \cdot \mathbb{E}(U_i). \tag{9}$$

B. Electricity Market Price and Bidding Curve

Day-ahead MCP and Real-time Market Price. At the time of making joint bidding and GLB decisions, MCPs of day-ahead markets in N regions are unknown. We model them as N independent random variables P_j ($j \in [1, N]$), each with probability distribution $f_{P_j}(p)$ that can be empirically estimated from historical data [7]. Here we assume that the CSP has negligible market power and its bidding and GLB behavior will not affect the dynamics of electricity markets.[2]

Similarly, the real-time market prices in N regions are also unknown when making bidding and GLB decisions. We

[2]The assumption is reasonable as, *e.g.*, datacenters in the US only consume 2% of total electricity [12], and it is usually used in the literature such as [32].

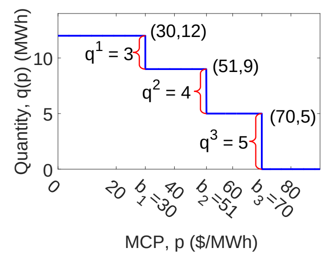

Fig. 5. An illustrating example for the (step-wise) bidding curve constructed from the submitted three bids in Fig. 3.

model the price of real-time market j as a random variable P_j^{RT} whose probability distribution can also be empirically estimated from historical data [7]. We define $\mu_j^{\mathsf{RT}} \triangleq \mathbb{E}[P_j^{\mathsf{RT}}]$ as the expectation of P_j^{RT}. We assume that all day-ahead MCPs P_j's and real-time market prices P_j^{RT}'s are independent.[3]

Bidding Curve. We explore the full design space of bidding strategy via *bidding curve*, which is a well-accepted concept in the power system community [13], [23]. Bidding curve, denoted as $q_j(p)$, is a function that maps the (realized) day-ahead market MCP to the amount of electricity the CSP wishes to obtain from day-ahead market j, by placing multiple bids. We remark that it is a common practice for one entity (*e.g.*, a utility company) to submit multiple bids to one electricity market.

Bidding curve is useful in designing bidding strategies in the following sense. First, any set of bids can be mapped to a bidding curve. Suppose the CSP submits K bids, namely$\left\langle b_j^k, q_j^k \right\rangle, k = 1, \ldots, K$, to the day-ahead market of region j, where b_j^k is the bidding price and q_j^k is the bidding quantity of the k-th bid. The corresponding bidding curve is a step-wise decreasing function as

$$q_j(p) = \sum_{k: b_j^k \geq p} q_j^k, \ \ \forall p \in \mathbb{R}^+. \tag{10}$$

For example, considering the three bids in Fig. 3, we can construct the corresponding bidding curve as shown in Fig. 5.

Recall that if day-ahead market MCP is p, then all bids whose bidding prices are higher than p will be accepted. Thus, the right hand side of (10) represents the total amount of electricity obtained when the day-ahead MCP is p. Clearly, the purchased amount will be non-increasing in MCP p. Thus, a valid bidding curve $q_j(p)$ must be a non-increasing function.

Second, any non-increasing function is a valid bidding curve and can be realized by placing a set of bids. For example, the bidding curve in (10) can be realized by placing the K bids $\left\langle b_j^k, q_j^k \right\rangle, k = 1, \ldots, K$ stated above.

Based on the above two observations, we design bidding strategy by choosing a bidding curve from the feasible set

$$\mathcal{Q} \triangleq \left\{ q(p) \mid q\left(p_1\right) \leq q\left(p_2\right), \forall p_1 \geq p_2, p_1, p_2 \in \mathbb{R}^+ \right\}. \tag{11}$$

Remark. In this paper, we assume that the CSP is allowed to submit any number, possibly infinite number, of bids. This

[3]We remark that this independence assumption may not hold in practice. But it significantly simplifies our analysis and allows us to reveal some important insights. A comprehensive study of considering correlations between day-ahead MCPs and real-time prices would be an interesting future work.

assumption allows us to significantly simplify the derivation of optimal solution to the joint bidding and GLB problem in Sec. IV. In Sec. VI, we discuss how to approximately realize a continuous bidding curve with a limited number of bids in the practical implementation. Our simulation results in Sec. VII (Tab. I) suggest that the performance loss due to the approximation error is minor.

Electricity Cost. Given the bidding curve $q_j(p)$ and the GLB decision $\boldsymbol{\alpha}$, we denote the *expected* electricity procurement cost of the CSP in electricity market j as $\mathsf{ECost}_j\left(q_j(p), \boldsymbol{\alpha}\right)$, which consists of settlement in both day-ahead trading and real-time trading.

- In day-ahead trading, suppose that the MCP in the day-ahead market j is p, the committed supply will be $q_j(p)$ and the day-ahead trading cost is $p \cdot q_j(p)$.
- In real-time trading, the day-ahead committed supply $q_j(p)$ may not exactly match the real-time demand V_j. If $V_j = v$ and $v > q_j(p)$, *under-supply* happens and we need to buy $v - q_j(p)$ amount of electricity at expected price μ_j^{RT}, so the expected cost due to under-supply would be $\mu_j^{\mathsf{RT}} \int_{q_j(p)}^{\bar{v}_j} \left(v - q_j(p)\right) f_{V_j}(v) dv$. Similarly, if *over-supply* happens, the unused electricity $(q_j(p) - v)$ will be sold back at a discounted price βp and the expected rebate due to over-supply is $\beta p \int_0^{q_j(p)} (q_j(p) - v) f_{V_j}(v) dv$. The expected real-time trading cost is simply the under-supply cost minus the over-supply rebate.

Based on the above analysis, we obtain the expression of $\mathsf{ECost}_j\left(q_j(p), \boldsymbol{\alpha}\right)$ in (12) by applying the total expectation theorem. Note that $\mathsf{ECost}_j\left(q_j(p), \boldsymbol{\alpha}\right)$ is related to the GLB decision $\boldsymbol{\alpha}$ through the distribution of V_j (the workload of datacenter j), which is computed by (7) and (8).

C. Problem Formulation

According to our investigations of some real-world pricing schemes, the bandwidth cost can be comparable to the electricity cost [41], so our objective is to minimize the summation of electricity cost and bandwidth cost. We now formulate the problem of joint bidding and GLB:

$$\begin{aligned} \textbf{P1:} \quad & \min \quad \sum_{j=1}^{N} \mathsf{ECost}_j\left(q_j(p), \boldsymbol{\alpha}\right) + \mathsf{BCost}(\boldsymbol{\alpha}) \\ & \text{var.} \quad \boldsymbol{\alpha} \in \mathcal{A}, q_j(p) \in \mathcal{Q}, j = 1, \ldots, N. \end{aligned}$$

where $\mathcal{A}$ is the set of all feasible GLB decisions, defined in (6) and $\mathcal{Q}$ is the set of all feasible bidding curves, defined in (11). It is straightforward to see both $\mathcal{A}$ and $\mathcal{Q}$ are convex sets. The objective is to minimize the summation of electricity cost of N datacenters and network cost, by optimizing bidding strategies and GLB decisions. The consideration of joint bidding and GLB as well as the market and demand uncertainty differentiates our work from existing works, *e.g.*, [7], [28], [29], [36]. We emphasize that it is important to consider input uncertainty to fully capitalize the economic benefit of joint bidding and GLB under real-world market mechanisms.

Challenges. There are two challenges in solving problem **P1**. First, it can be shown that the objective function of **P1** is non-convex with respective to $q_j(p)$ (see our technical report [41]). Second, the optimization variable $q_j(p)$ is a functional variable with infinite dimensions. Thus it is highly non-trivial to solve this non-convex infinite-dimensional problem optimally by existing solvers, without incurring forbidden complexity.

IV. An Optimal Joint Bidding and GLB Solution

In this section, we design an algorithm to solve the challenging problem **P1** optimally and efficiently.

A. Reducing P1 to a Convex Problem and Approach Sketch

To begin with, we define a sub-region of $\mathcal{Q}$ as follows

$$\hat{\mathcal{Q}}_j = \{q_j(p) | q_j(p) \in \mathcal{Q}, \text{ and } q_j(p) = 0, \forall p \geq \mu_j^{\mathsf{RT}}\}. \quad (13)$$

As compared to $\mathcal{Q}$ defined in (11), the new constraint in the definition of $\hat{\mathcal{Q}}_j$, *i.e.*, $q_j(p) = 0, \forall p \geq \mu_j^{\mathsf{RT}}$, means that we do not submit any bid to day-ahead market j with bidding price higher than μ_j^{RT}, *i.e.*, the expected price of real-time market j. It is easy to verify that both $\mathcal{Q}$ and $\hat{\mathcal{Q}}_j$ are convex sets.

Theorem 1: The following problem **P2** is *convex* and has the same optimal solution as **P1**:

$$\begin{aligned} \textbf{P2:} \quad & \min \quad \sum_{j=1}^{N} \mathsf{ECost}_j\left(q_j(p), \boldsymbol{\alpha}\right) + \mathsf{BCost}(\boldsymbol{\alpha}) \\ & \text{var.} \quad \boldsymbol{\alpha} \in \mathcal{A}, \ q_j(p) \in \hat{\mathcal{Q}}_j, j = 1, \ldots, N. \end{aligned}$$

Remarks. (i) Problems **P1** and **P2** differ only in the feasible set of bidding curve $q_j(p)$. It is $\mathcal{Q}$ in **P1** but $\hat{\mathcal{Q}}_j$ in **P2**. The objective function is nonconvex over $\mathcal{Q}$ but convex over $\hat{\mathcal{Q}}_j$, as shown in the proof of Theorem 1 in Appendix A; hence, **P1** is a nonconvex problem but **P2** now is a convex one. (ii) Intuitively, the optimal bidding curve for day-ahead market j must be in $\hat{\mathcal{Q}}_j$. This is because the CSP can always buy electricity from real-time market j at an expected price μ_j^{RT}; thus it is not economic to submit bids with bidding price higher than μ_j^{RT} to day-ahead market j. Such bidding strategies must be in set $\hat{\mathcal{Q}}_j$, defined in (13).

Theorem 1 allows us to solve **P1** by solving the convex problem **P2**. However, **P2** still suffers the infinite-dimension challenge, since optimizing bidding curves in general requires us to specify the value of $q_j(p)$ for every $p \in [0, \mu_j^{\mathsf{RT}})$. To illustrate our design, we first rewrite problem **P2**,

$$\begin{aligned} & \min_{\boldsymbol{\alpha} \in \mathcal{A}} \min_{q_j(p) \in \hat{\mathcal{Q}}_j, \forall j} \left\{ \sum_{j=1}^{N} \mathsf{ECost}_j\left(q_j(p), \boldsymbol{\alpha}\right) + \mathsf{BCost}(\boldsymbol{\alpha}) \right\} \\ = & \underbrace{\min_{\boldsymbol{\alpha} \in \mathcal{A}} \left\{ \sum_{j=1}^{N} \underbrace{\left[\min_{q_j(p) \in \hat{\mathcal{Q}}_j} \mathsf{ECost}_j\left(q_j(p), \boldsymbol{\alpha}\right) \right]}_{\text{Problem } \mathbf{EP}_j(\boldsymbol{\alpha}) \text{, solved in Sec. IV-B}} + \mathsf{BCost}(\boldsymbol{\alpha}) \right\}}_{\text{Problem } \mathbf{P3} \text{, solved in Sec. IV-C}} \end{aligned} \quad (14)$$

The structure of the expression in (14) suggests a nested-loop approach to solve problem **P2**.

$$\mathsf{ECost}_j\left(q_j(p),\boldsymbol{\alpha}\right)=\int_0^{+\infty}f_{P_j}(p)\,\underbrace{[\,\underbrace{pq_j(p)}_{\substack{\text{Day-ahead}\\ \text{trading cost}}}\underbrace{-\underbrace{\beta p\int_0^{q_j(p)}(q_j(p)-v)f_{V_j}(v)dv}_{\text{Rebate of over-supply}}+\underbrace{\mu_j^{\mathsf{RT}}\int_{q_j(p)}^{\bar{v}_j}(v-q_j(p))f_{V_j}(v)dv}_{\text{Cost of under-supply}}}_{\text{Real-time trading cost}}\,]}_{\text{Expected electricity cost of datacenter } j \text{ conditioning on day-ahead market } j\text{'s MCP } P_j=p}\,dp. \quad (12)$$

- *Inner Loop:* The CSP optimizes its bidding strategies for each regional day-ahead market with given GLB decision $\boldsymbol{\alpha}$, by solving the following problems:

$$\mathbf{EP}_j(\boldsymbol{\alpha}):\quad \min_{q_j(p)\in\hat{\mathcal{Q}}_j}\mathsf{ECost}_j\left(q_j(p),\boldsymbol{\alpha}\right),\ \ j=1,\ldots,N.$$

- *Outer Loop:* After solving the inner-loop problems $\mathbf{EP}_j(\boldsymbol{\alpha})$ and obtaining the optimal bidding curves, denoted by $q_j^*(p;\boldsymbol{\alpha})$, $\forall j=1,\ldots,N$, the CSP optimizes the (finite-dimensional) GLB decision $\boldsymbol{\alpha}$ by solving the following problem:

$$\textbf{P3:}\quad \min_{\boldsymbol{\alpha}\in\mathcal{A}}\quad \sum_{j=1}^{N}\mathsf{ECost}_j\left(q_j^*(p;\boldsymbol{\alpha}),\boldsymbol{\alpha}\right)+\mathsf{BCost}(\boldsymbol{\alpha}).$$

In our technical report [41], we prove that the inner-loop problem $\mathbf{EP}_j(\boldsymbol{\alpha})$ and outer-loop problem **P3** are both convex, which are perhaps not surprising. In the next two subsections, we solve $\mathbf{EP}_j(\boldsymbol{\alpha})$ and **P3** to obtain an optimal joint bidding and GLB solution to **P2**, which is also optimal for **P1**.

B. Inner Loop: Optimal Bidding Given GLB Decision

The inner-loop problem $\mathbf{EP}_j(\boldsymbol{\alpha})$ is concerned about designing optimal bidding strategy for day-ahead market in region j (by choosing $q_j(p)\in\hat{\mathcal{Q}}_j$) with GLB decision $\boldsymbol{\alpha}$ given, in face of demand and price uncertainty. Note that $\mathbf{EP}_j(\boldsymbol{\alpha})$ is closely related to the classic Newsvendor problem [19]. In the Newsvendor problem, the market prices are given and only the buying quantity should be optimized under demand uncertainty, while in $\mathbf{EP}_j(\boldsymbol{\alpha})$ we need to optimize both the bidding quantities and bidding prices simultaneously under both price and demand uncertainties.

Let the cumulative distribution function (CDF) of V_j, *i.e.*, the demand of datacenter j, be $F_{V_j}(x)\triangleq\int_0^x f_{V_j}(v)dv$, where $f_{V_j}(v)$ is PDF of V_j given in (7). The following theorem shows that $\mathbf{EP}_j(\boldsymbol{\alpha})$ admits a closed-form solution $q_j^*(p;\boldsymbol{\alpha})$, addressing the infinite-dimension challenge.

Theorem 2: Given GLB decision $\boldsymbol{\alpha}$, we assume that $F_{V_j}(x)$ is strictly increasing; thus its inverse exists and is denoted as $F_{V_j}^{-1}(x)$. The optimal bidding curve for solving $\mathbf{EP}_j(\boldsymbol{\alpha})$ is given by, for $j=1,\ldots,N$,

$$q_j^*(p;\boldsymbol{\alpha})=\begin{cases}F_{V_j}^{-1}\left(\frac{\mu_j^{\mathsf{RT}}-p}{\mu_j^{\mathsf{RT}}-\beta p}\right), & \text{if } p\in\left[0,\mu_j^{\mathsf{RT}}\right);\\ 0, & \text{otherwise.}\end{cases}\qquad (15)$$

The proof of Theorem 2 is delegated in Appendix B. The optimal bidding curve $q_j^*(p;\boldsymbol{\alpha})$ is *universal* in that it does not depend on the distribution of day-ahead MCP P_j. This is because $q_j^*(p;\boldsymbol{\alpha})$ actually minimizes the expected electricity procurement cost for any p. It is easy to extend this result to the general non-decreasing $F_{V_j}(x)$ [41].

Remarks. The optimal bidding curve $q_j^*(p;\boldsymbol{\alpha})$ in (15) is a decreasing function in the day-ahead MCP p. This meets our intuition that a good bidding strategy should purchase more electricity when p is low and less electricity when p is high. Similarly, it also meets our intuition that $q_j^*(p;\boldsymbol{\alpha})$ increases in the sell-back discounting factor β. A larger β means less penalty of over-supply, thus the CSP should bid for more electricity from the day-ahead market to balance the penalty of under-supply. By taking into account both the demand statistics ($F_{V_j}(\cdot)$) and market condition (p and β), $q_j^*(p;\boldsymbol{\alpha})$ achieves the best balance between over-supply and under-supply to minimize the expected electricity cost, and allows our overall solution to be robust to demand uncertainty, as shown in our case study in Fig. 1(a) as well as simulation results in Sec. V. We provide more insightful discussions in Sec. V.

C. Outer Loop: Optimal GLB with Optimal Bidding Curve as a Function of GLB Decision

After obtaining the optimal bidding strategy $q_j^*(p;\boldsymbol{\alpha})$ as a function of GLB decision $\boldsymbol{\alpha}$, we now solve the outer-loop problem **P3** for optimizing GLB. While **P3** is convex and of finite dimension, its objective function does not admit an explicit-form expression since we do not have an explicit expression of the optimal objective value of $\mathbf{EP}_j(\boldsymbol{\alpha})$. Thus, gradient-based algorithms cannot be directly applied.

We tackle this issue by adapting a zero-order optimization algorithm, named General Pattern Search (GPS) [21], to solve the out-loop problem without knowing explicit expression of the objective function. *Zero-order optimization algorithms* are widely used to solve optimization problems without directly accessing the derivative information. The GPS algorithm in [21] is a popular zero-order optimization algorithm for solving problems with linear constraints, which is suitable for **P3**.

Our adapted GPS algorithm is an iterative algorithm. In each iteration, the algorithm first creates a set of searching directions, named "patterns", which *positively spans* the entire feasible set. It then searches the directions one by one in order to find a direction, along which the objective value decreases. And we will update to a better solution if we find one. In each search, the algorithm needs to evaluate the objective value of $\mathbf{EP}_j(\boldsymbol{\alpha})$ given a GLB decision $\boldsymbol{\alpha}$, which can be obtained by plugging the optimal solution $q_j^*(p;\boldsymbol{\alpha})$ into the objective function of $\mathbf{EP}_j(\boldsymbol{\alpha})$. In this manner, our adapted GPS algorithm works like gradient-based algorithms, but without the need to compute gradient/subgradient. We summarize our proposed nested-loop algorithm in Algorithm 1.

Algorithm 1 An Algorithm for Solving **P3** Optimally

initialize $\boldsymbol{\alpha}^0 \leftarrow \mathbf{I}_{N\times N}$, $t \leftarrow 0$
while not converge **do**
  `current_value` $\leftarrow$ **P3-Obj**$(\boldsymbol{\alpha}^t)$
  Get $\boldsymbol{\alpha}^{t+1}$ by invoking **P3-Obj** and comparing with `current_value` at most $2N^2$ times (see [21, Fig. 3.4])
  $t \leftarrow t+1$
end while
$\boldsymbol{\alpha}^* \leftarrow \boldsymbol{\alpha}^t$
Compute $q_j^*(p;\boldsymbol{\alpha}^*)$ by (15) for all $j \in [1,N]$
return $\boldsymbol{\alpha}^*, q_j^*(p;\boldsymbol{\alpha}^*)$ for all $j \in [1,N]$

A subroutine to compute the objective value of P3

function **P3-OBJ**$(\boldsymbol{\alpha})$
  initialize $j \leftarrow 1$, val $\leftarrow \mathsf{BCost}(\boldsymbol{\alpha})$ by (9)
  while $j \leq N$ **do**
    Compute $q_j^*(p;\boldsymbol{\alpha})$ by (15)
    `val` $\leftarrow$ `val` $+ \mathsf{ECost}_j\left(q_j^*(p;\boldsymbol{\alpha}),\boldsymbol{\alpha}\right)$ by (12)
    $j \leftarrow j+1$
  end while
  return `val`
end function

In general, GPS algorithm is not guaranteed to converge to the globally optimal solution [21]. In the following theorem, we prove that our Algorithm 1 actually converges to the optimal solution to the convex problem **P3**, under proper conditions.

Theorem 3: Assume that $f_{U_j}(u)$, $j = 1,\ldots,N$, are differentiable and their derivatives are continuous. Algorithm 1 converges to a globally optimal solution to **P3**, which is also an optimal solution to **P1** and **P2**.

Remarks. Theorem. 3 follows the facts that **P3** is convex and GPS algorithm converges to a point satisfying the KKT condition [21]. The proof is deferred in [41] due to space limitation.

D. Complexity and Practical Considerations

In this section, we discuss the computation complexity and some practical considerations for our solution.

1) Computational Complexity: In our model and analysis, we assume that both MCP P_j and the demand U_j are continuous random variables. When applying them to practice, we need to sample a PDF (which is a continuous function) into a probability mass function (which is a discrete sequence). So we assume that we sample both the PDF of P_j, *i.e.*, $f_{P_j}(p)$, and the PDF of U_j, *i.e.*, $f_{U_j}(v)$, into sequences with length m. The value of m depends on both the ranges of MCP and demand and the accuracy we aim to achieve. Based on such sampling, we show the computational complexity of our proposed solution, *i.e.*, Algorithm 1.

Theorem 4: If Algorithm 1 converges in n_{iter} iterations, its time complexity is $O(n_{\mathsf{iter}}((N^5 m \log(Nm) + N^3 m^2)))$.

The proof of Theorem 4 is in Appendix C. The complexity is linear with the number of iterations until convergence. However, exactly characterizing the convergence rate of GPS algorithm is still an open problem [10], and thus it is hard to get sharp bounds for the number of iterations, *i.e.*, n_{iter}. Instead, we empirically evaluate the convergence rate of our Algorithm 1 in Sec. VII-D. The results show that our Algorithm 1 converges fast – within 30 iterations – for the practical setting considered (*i.e.*, $n_{\mathsf{iter}} \leq 30$).

The highest-order parameter for the complexity is N, *i.e.*, the number of datacenters of the CSP.But in reality N is usually small: For example, there are only 10 deregulated electricity markets in US. Thus, Theorem 4 shows that the complexity of our Algorithm 1 is affordable in practice.

2) Imperfect Probability Distributions.: In our model and solution, we require perfect probability distributions of day-ahead MCP P_j and the regional demand U_j. However, in practice, learning distributions from historical data inevitably introduces certain estimation error. Thus it is important to evaluate the robustness of our solution to the estimation error. In Sec.V, we empirically show that our solution works pretty well for *imperfect* probability distributions of the demand U_j which only use the first-order (expectation) and second-order (variance) statistic information.

V. Impacts of Demand and Price Uncertainty

In this section, we study the impacts of demand and price uncertainties, to better understand the observations in Fig. 1(a) and 1(b). We will use the variance of a random variable to measure its uncertainty.[4] Taking normal distribution as an example, the distribution of a random variable with a larger variance will be more "stretched" and it is more likely to take very large or small values.

Unless otherwise specified, our discussions in this section involve a single datacenter.

A. Impact of Demand Uncertainty

Demand uncertainty is one of the main challenges handled by this work and it is interesting to ask how the performance will change with different levels of demand uncertainty. Given any purchased amount of electricity from the day-ahead market, a larger demand uncertainty will increase the possibility of real-time mismatch. As elaborated in Sec. II, both over-supply and under-supply will introduce inefficiency to the market and incur additional cost. Thus, the demand uncertainty is always an unwished curse to increase the electricity cost, even for our carefully designed bidding strategy.

Now, we formalize our statement in Lemma 1.

***Lemma** 1:* Assume that the day-ahead MCP is positive and follows an arbitrary distribution, and that the electricity demand (proportional to workload) follows Truncated Normal, Gamma, or Uniform distribution, with a variance σ_D^2. The optimal expected electricity cost, achievable by using the strategy in (15), is non-decreasing in σ_D^2.

The proof of Lemma 1 is in Appendix D. Though $q_j^*(p;\boldsymbol{\alpha})$ in (15) cannot fully eliminate this curse, it can handle the demand uncertainty carefully such that the performance will

[4] We remark that Lemma 1 and 2 developed in this section still hold without the assumption of specific distributions but using the "increasing convex ordering" or "variability ordering" defined in [34] to measure the uncertainties. See our discussions in [41].

not deteriorate too much, as illustrated in the empirical studies in Fig. 1(a) and Fig. 10.

B. Impact of Price Uncertainty

The price uncertainty in the day-ahead market is the fundamental reason to motivate the continuous bidding curve design and differentiates $\mathbf{EP}_j(\boldsymbol{\alpha})$ in this paper from the classic Newsvendor problem [19]. Different from demand uncertainty, uncertainty in MCP of day-ahead market allows the optimal bidding curve $q_j^*(p;\boldsymbol{\alpha})$ to save cost. In particular, the unique two-sequential-market structure where the real-time market serves as a backup for the day-ahead market allows our bidding strategy $q_j^*(p;\boldsymbol{\alpha})$ to fully explore the benefit of low MCP values but control the risk of high MCP values. We elaborate as follows. When MCP fluctuates, its value, denoted by p, takes small and large values. When p is small, we can purchase cheap electricity from the day-ahead market and thus enjoys "gain". When p is large, we have to purchase expensive electricity from the day-ahead market and thus suffers "loss". However, when $p \geq \mu_j^{\mathsf{RT}}$, our optimal bidding strategy $q_j^*(p;\boldsymbol{\alpha})$ will not purchase any electricity from the day-ahead market but purchase all electricity from the real-time market at the expected price μ_j^{RT}, bounding the "loss" due to high MCP values. Overall, the gain out-weights the loss and we achieve cost saving by leveraging MCP uncertainty. In fact, the larger the MCP uncertainty, the more significant the saving, as illustrated in our case study in Fig. 1(b).

Now, we make the above intuitive explanations more rigorous in Lemma 2.

Lemma 2: Assume that the electricity demand (proportional to workload) is positive and follows an arbitrary distribution, and that the day-ahead MCP follows Truncated Normal, Gamma, or Uniform distribution, with a variance σ_P^2. The optimal expected electricity cost, achievable by using the strategy in (15), is non-inceasing in σ_P^2.

The proof for Lemma 2 is in Appendix E. It implies that a larger price uncertainty in the day-ahead market will bring more benefit of the two-stage market structure and decrease the cost expectation.

VI. Bidding with Finite Bids

We remark that the previously demonstrated advantages can only be realized when submitting an infinite number of bids or a continuous bidding curve is allowed. If not, its feasibility to solve practical problems can be questioned. In this part, we want to adapt our previous design to tackle the problem when only K bids $(b^k, q^k), k = 1, \ldots, K$ can be submitted.

Recall that the bid (b^k, q^k) succeeds only when the MCP of the day-ahead market is lower than or equal to the bidding price b^k. Implicitly, submitting K bids $(b^k, q^k), k = 1, \ldots, K$ can be viewed as proposing a step-wise bidding curve

$$\bar{q}(p) = \sum_{k: b^k \geq p} q^k.$$

Our task in this section is to optimize $\bar{q}(p)$, *i.e.*, the values of $b^k, q^k, \forall k$, to minimize the electricity cost expectation.

A. Performance Loss Characterization

Firstly, we characterize the cost difference of two different bidding curves by the following lemma.

Lemma 3: When the day-ahead MCP distribution for electricity market is given as $f_{P_j}(p)$ and we denote the costs of two bidding curves $q^1(p), q^2(p)$ $(q^1(p) = q^2(p) = 0, \text{ for } p \geq \mu_j^{\mathsf{RT}})$ as $\mathsf{ECost}_j\left(q^1(p)\right), \mathsf{ECost}_j\left(q^2(p)\right)$, [5] respectively, we can have

$$\begin{aligned} &|\mathsf{ECost}_j\left(q^1(p)\right) - \mathsf{ECost}_j\left(q^2(p)\right)|^2 \\ \leq\ & \mathcal{M} \cdot \int_0^{\mu_j^{\mathsf{RT}}} |q^1(p) - q^2(p)|^2 dp, \end{aligned}$$

where $\mathcal{M} = \int_0^{\mu_j^{\mathsf{RT}}} \left[f_{P_j}(p)(2\mu_j^{\mathsf{RT}} - \beta p - p)\right]^2 dp$ is a constant determined by the market condition and irrelevant to the bidding curves.

Essentially Lemma 3 shows that if two bidding curves are close in terms of the distance $\int_0^{\mu_j^{\mathsf{RT}}} |q^1(p) - q^2(p)|^2 dp$, their expected costs are also close, which is quite intuitive. The proof of Lemma 3 is in Appendix F.

We denote the optimal bidding curve in (15) and its cost by $q^*(p)$ and C^*. Obviously, C^* serves as a lower bound for $\mathsf{ECost}(\bar{q}(p))$.[6] By applying Lemma 3, we can have

$$\mathsf{ECost}_j(\bar{q}(p)) - C^* \leq \sqrt{\mathcal{M} \cdot \int_0^{\mu_j^{\mathsf{RT}}} |q^*(p) - \bar{q}(p)|^2 dp}. \quad (16)$$

Remarks. (a) This result guarantees that the performance loss compared with the optimal bidding curve by submitting only K bids is upper bounded. And the upper bound is jointly determined by the market condition ($\mathcal{M}$) and how the bids are designed ($\int_0^{\mu_j^{\mathsf{RT}}} |q^*(p) - \bar{q}(p)|^2 dp$). (b) (16) also suggests a guideline for designing a "good" step-wise bidding curve: we seek a $\bar{q}(p)$ with a small value of $\int_0^{\mu_j^{\mathsf{RT}}} |q^*(p) - \bar{q}(p)|^2 dp$. Alternatively speaking, we need to find a stepwise function to approximate the continuous bidding curve.

B. Step-wise Bidding Curve Design

Without loss of generality, we assume that the bidding prices are indexed increasingly with $b^k \leq b^{k+1}$ and $b^0 = 0, b^{K+1} = \mu_j^{\mathsf{RT}}$. Thus when $p \in (b^k, b^{k+1}]$, we have $\bar{q}(p) = \sum_{l=k+1}^{K} q^l$. To have a good step-wise bidding curve, it is natural to find a $\bar{q}(p)$ to minimize $\int_0^{\mu_j^{\mathsf{RT}}} |q^*(p) - \bar{q}(p)|^2 dp$, *i.e.*, to solve the following problem,

$$\begin{aligned} \textbf{FB} \quad \min \quad & \sum_{k=0}^{K} \int_{b_k}^{b^{k+1}} |q^*(p) - \sum_{l=k+1}^{K} q^l|^2 dp && (17a) \\ \text{s.t.} \quad & b^k \leq b^{k+1} && (17b) \\ & q^k \geq 0 && (17c) \\ \text{var.} \quad & b^k, q^k, k = 1 \ldots, K. && (17d) \end{aligned}$$

According to (16), any algorithm to produce a solution with a small objective value of **FB** can produce a set of bids with

[5] Since we consider only bidding strategy here, the GLB-related parameter $\boldsymbol{\alpha}$ is ignored to simplify the notation.

[6] C^* can be viewed as the optimal value of the cost minimization problem without the "finite-bid" constraint.

Algorithm 2 A Heuristic Algorithm for Solving **FB**

Input: Optimal bidding curve $q^*(p)$, number of bids K.
Output: $(b^k, q^k), k = 1, \ldots, K$.

1: **initialize** $(b^k, q^k), k = 1, \ldots, K$.
2: **while** not converge **do**
3: **for** $k = 1, \ldots, K$ **do**
4: Find a value $\tilde{b^k}$ that satisfies
$$2q^*(\tilde{b^k}) - \frac{1}{b^{k+1} - \tilde{b^k}} \int_{\tilde{b^k}}^{b^{k+1}} q^*(p)dp - \frac{1}{\tilde{b^k} - b^{k-1}} \int_{\tilde{b^k}}^{b^{k+1}} q^*(p)dp = 0$$
by binary search.
5: Update $b^k = \tilde{b^k}$ if $\tilde{b^k}$ decreases the objective value of (17a).
6: **end for**
7: **end while**
8: $s^{k+1} = \frac{1}{b^{k+1} - b^k} \int_{b^k}^{b^{k+1}} q^*(p)dp, \forall k$.
9: $q^k = s^k - s^{k+1}, \forall k$
10: **return** $(b^k, q^k), k = 1, \ldots, K$.

low cost expectation. But unfortunately, **FB** is nonconvex and the global optimal solution is difficult to obtain. Apart from the off-the-shelf solvers, we provide a heuristic algorithm in Alg. 2 to solve **FB** iteratively. The detailed analysis of Alg. 2 is relegated in [41] to due to the space limitation and we only provide the following proposition on its convergence property.

***Proposition** 1:* The objective value of **FB** is non-increasing in each iteration and thus Alg. 2 will converge.

The correctness of Proposition 1 is guaranteed by the facts that the objective value is non-increasing (Line 5 of Alg. 2) and that the optimal objective value of **FB** is lower bounded by 0. The proof is omitted.

Back to our joint optimization framework to meet the finite-bid constraint, we can firstly ignore it and adopt Alg. 1 to produce the optimal, yet possibly continuous, bidding curves $q_j^*(p; \boldsymbol{\alpha}^*), \forall j$. After that, we use Alg. 2 to produce step-wise bidding curves $\bar{q}_j(p)$ to approximate $q_j^*(p; \boldsymbol{\alpha}^*)$ for different datacenters. Obviously the objective value by $q_j^*(p; \boldsymbol{\alpha}^*)$ is a lower bound for the optimal value of the problem with finite-bid constraints. Then, according to (16), if $\bar{q}_j(p)$ is close to $q_j^*(p; \boldsymbol{\alpha}^*)$ for all j, the objective value in terms of $q_j^*(p; \boldsymbol{\alpha}^*), \forall j$ is also close to the optimal value.

VII. Empirical Evaluations

In this section, we use trace-driven simulations to evaluate the performance of our proposed solution.

A. Dataset and Settings

Network Settings. We consider a CSP operating 3 datacenters in San Diego, Houston, and New York City. We assume that due to quality of experience consideration, the CSP cannot balance workloads between datacenters in San Diego and New York City. We set the unit bandwidth cost of routing workloads across datacenters as $z_{ij} = \kappa \cdot \left(\mu_1^{\mathsf{RT}} + \mu_2^{\mathsf{RT}} + \mu_3^{\mathsf{RT}}\right)/3$ if $i \neq j$, and $z_{ii} = 0$, $i = 1, 2, 3$. We let $\kappa = 0.1$ as a default setting, and we vary the values of κ to evaluate the overall cost-saving performance under different bandwidth-cost settings.

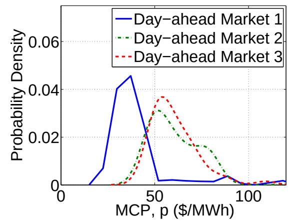

Fig. 6. Empirical distributions of MCPs, 2pm.

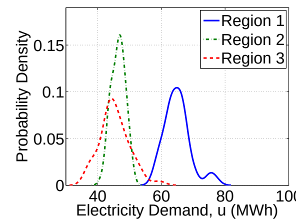

Fig. 7. Empirical distributions of electricity demands, 2pm.

Workload and Electricity Demand. We get the numbers of service requests per hour against the Akamai CDN in North America for 48 days from Akamai's Internet Observatory website [1]. By using the conversion ratio claimed by Google for its datacenters [28], we scale up the request information to create an electricity demand series with averaged hourly demand of 125 MWh. The total demand is divided into three regions according to regional electricity consumptions of the three locations [41]. We set the ratio of demand of region i to be served locally, *i.e.*, λ_i, to be 0.7. We also set datacenter j's capacity C_j to be 30% larger than region j's peak demand, since it was reported that on average 30% or more of the capacity of datacenters is idling in operation [7], [12].

Electricity Prices in Day-ahead and Real-time Markets. We obtain the electricity prices (MCP of day-ahead market and real-time market price) from three regional ISO websites which serve the customers in San Diego, Houston, and New York, respectively [6] [11] [26]. The discounting factor β of selling back unused electricity is set as 0.5, which means that the CSP suffers half loss in case of over-supply.

Evaluation and Comparison. We test our design on 24 instances, each corresponding to one hour of the day. For each hour, the distributions of electricity demand, day-ahead MCP and real-time prices are learned from our dataset, and the real-time price expectation is computed from the distribution accordingly. For illustration purpose, we plot the empirical distributions of MCPs and demands for 2pm in Fig. 6 and Fig. 7, respectively. We denote our solution as OptBidding-OptGLB, in which the GPS part is based on an implementation used in [8], [9]. We test the following four baseline alternatives. (i) NoBidding-NoGLB: it represents the strategy of buying all electricity in real-time markets without doing GLB. It serves as the *benchmark* to compute cost reduction for other algorithms. (ii) OptBidding-NoGLB: it represents the strategy of optimally bidding in day-ahead markets but without doing GLB. (iii) NoBidding-OptGLB: it represents the strategy of doing no bidding in the day-ahead markets but purchasing all electricity in real-time markets and doing optimal GLB (adapted from the solution in [32]). (iv) SimpleBidding-OptGLB: it represents a joint bidding and GLB strategy proposed in [7], in which the CSP only submits one bid to each day-ahead market j with bidding price being μ_j^{RT} and the GLB strategy is optimized by a Matlab solver *fmincon*.

B. Performance Comparison and Impact of Finite Bids

We compare the performance of different solutions in terms of the expected daily cost in Tab. I. Further, we also evaluate

TABLE I
Cost-saving performance of different schemes.

Solution	Daily Cost (k$)	Reduction (%)
NoBidding-NoGLB	161.9	-
NoBidding-OptGLB (adapted from [32])	154.5	4.6
SimpleBidding-OptGLB [7]	155.8	3.8
OptBidding-NoGLB	135.4	16.4
OptBidding-OptGLB (Our solution)	128.2	**20.8**
OptBidding-OptGLB (1 bid)	133.3	**17.7**
OptBidding-OptGLB (3 bids)	128.6	**20.5**

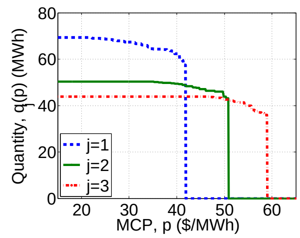

Fig. 8. Optimal bidding curves for three day-ahead markets, 4pm.

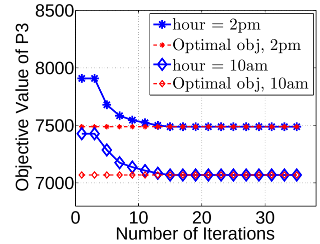

Fig. 9. Objective values in each iteration of our Algorithm 1.

the performance loss due to that we approximate the optimal bidding curve (which may require the CSP to submit infinite number of bids) by using only 1 and 3 bids in our solution. We show the cost reduction of using infinite number of bids, 1 bid, and 3 bids in the last three rows of Tab. I, respectively.

We have the following observations. First of all, as seen from Tab. I, we can see that our proposed solution outperforms all other alternatives and reduces the CSP's operating cost by 20.8% as compared to the benchmark NoBidding-NoGLB. Meanwhile, we observe that SimpleBidding-OptGLB only reduces the cost by 3.8%, which is much less than that achieved by our solution OptBidding-OptGLB. Moreover, the cost reduction (3.8%) is even less than NoBidding-OptGLB (4.6%), which does not perform bidding in the day-ahead markets but purchases all electricity from the real-time markets. This highlights the importance of designing intelligent strategies for bidding on the day-ahead markets.

In addition to intelligent bidding strategy design, we observe that GLB also brings extra cost saving for CSP. For example, NoBidding-OptGLB reduces the cost by 4.6% as compared to NoBidding-NoGLB, and OptBidding-OptGLB achieves 4.4% extra reduction as compared to OptBidding-NoGLB.

Here, we use the simple method explained in Sec. VI to approximate the optimal bidding curve with a finite number of bids (in particular, 1 and 3 bids in this experiment). From the last two rows in Tab. I, we observe that submitting 1 bid can achieve reasonably good performance (17.7% vs 20.8%). Submitting 3 bids can almost achieve the same performance as submitting infinite number of bids (20.5% vs 20.8%). This observation suggests that our solution performs well in practice even if the CSP is only allowed to submit a small number of bids to a day-ahead market. To understand this observation, we visualize the optimal bidding curves of three datacenters for one optimization instance (4pm) in Fig. 8. We can see that all three bidding curves are "flat" and thus can be accurately approximated by step-wise functions corresponding to submitting only a small number of bids.

C. Impact of Market Price Uncertainty and Demand Uncertainty

In Sec. I, we provide two experiments related to the electricity demand uncertainty and market price uncertainty (Fig. 1(a) and Fig. 1(b)) to motivate the study in this paper and we describe the details here. Our Solution denotes the strategy by OptBidding-OptGLB and **Baseline** denotes a simple strategy: in each region, we pick only one market with cheaper electricity, day-ahead market or real-time market depending on the price expectations, and buy the expected amount of electricity demand in the picked market (If picking the real-time market, we submit no bid in the day-ahead market; if picking the day-ahead market, we submit one bid with the bidding price infinity and the bidding quantity as the expected electricity demand). To understand their individual impact separately, we construct two experiments.

In Fig. 1(a), we set the day-ahead MCP and real-time price to be constant (their sample means), and test the performance of our solution and the baseline with different levels of demand uncertainty (we manipulate the data such that the demand expectations stay the same and their sample STDs increase from 0 to 4.2, where 0 STD represents the scenario without demand uncertainty.). As we can observe, the cost reduction ratio of our solution decreases from 7% to 6.7% while that of the baseline solution decreases from 7% to 5.5%, which fits our analysis in Sec. V-A. It also means that even though the demand uncertainty curses the performance of both two schemes, our solution behaves more robustly. In Fig. 1(b), we set the electricity demand to be constant (its sample mean), and test the performance with different levels of market price uncertainty (similarly, we keep the day-ahead MCP expectation the same and increase its sample STD from 0 to 30.). In this case, the performance of the baseline solution stays the same. This observation is not surprising because the baseline's decision will be the same for any level of market price uncertainty and we also only care about the expected cost. On the other hand, the cost reduction ratio of our solution increases from 7% to 21%. Also, this result should not be surprising based on our analysis in Sec. V-B.

D. Convergence Rate of the Joint Bidding and GLB Algorithm

In this subsection, we empirically evaluate the convergence rate of our proposed Algorithm 1. We run our algorithm for two instances with workload/price distribution of 10am and 2pm, respectively. From Fig. 9, we can see that our algorithm converges rather fast – within 30 iterations. The computation complexity of each iteration is polynomial in the problem size (Theorem 4). The main efforts in each iteration are just put to evaluate the objective values by a given set of candidate solutions, and the number of such candidate solutions is less than 18 (2 times the dimensions of $\boldsymbol{\alpha}$).

E. Impact of Inaccurate Demand Distribution Estimation

We properly scale the electricity demand of all three regions such that the demand expectations stay the same and the average of the normalized sample standard deviations among all three regions changes from 0.02 to 0.13, to mimic low to high uncertainty in workloads and hence electricity demand. Here normalized sample standard deviation is defined as the ratio of the sample standard deviation to the sample mean. We apply our solution OptBidding-OptGLB to the set of scaled demands and plot the cost reduction in Fig. 10. From Fig. 10, similar to the observations obtained in Sec. VII-C but using real-world data traces, we can see that the cost reduction decreases as the demand uncertainty increases, but the performance loss is minor, suggesting that our solution OptBidding-OptGLB is robust to demand uncertainty.

The main purpose of the experiments in this subsection is to study the impact of imperfect distribution estimation. In our solution OptBidding-OptGLB, we use the distribution of the demand U_j for region j as input. In practice, however, the CSP may not have the exact demand distributions, but just their estimates based on historical data. It is common for these estimated distributions to have the same mean and variance as the actual demand distributions, but it is difficult, if not impossible, for the estimated distribution to match the actual distribution exactly. A central question is then how sensitive is the performance of our solution OptBidding-OptGLB to the accuracy of the distribution estimation, given that we have obtained an accurate estimate of the mean and variance?

We explore answers to this question by comparing the performance achieved by our solution OptBidding-OptGLB based on the following distributions for demand with the same mean and variance: actual distribution, *normal distribution*, and *uniform distribution*. We compare their cost reductions in Fig. 10. As seen, the performance loss is minor, implying that accurate first and second order statistics of the demand distribution may be enough to determine the performance of our solution OptBidding-OptGLB. This observation also suggests an interesting direction for future work.

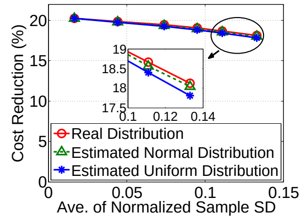

Fig. 10. Cost reductions with different levels of demand uncertainty and different estimated distributions.

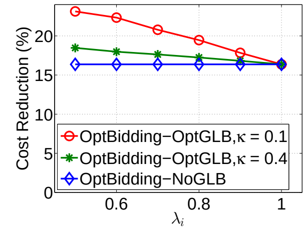

Fig. 11. Cost reductions when more workloads must be locally served, under different bandwidth cost.

F. Impact of Local Service Requirement and Bandwidth Cost

We investigate the impact of local service requirement, where we changes the percentage of demand that must be served locally, *i.e.*, λ_i, from 0.5 to 1.0. The simulation results are in Fig. 11, where we can see the cost reduction of our solution OptBidding-OptGLB decreases as λ_i increases. This matches our intuition that larger λ_i means that the CSP has less room to do GLB. When $\lambda_i = 1$, *i.e.*, all demand should be served locally, our solution OptBidding-OptGLB coincides with OptBidding-NoGLB.

We also study the impact of bandwidth cost, where we choose two different values (0.1 and 0.4) for the bandwidth cost factor κ. We show the cost reduction in Fig. 11. As seen, a larger κ, meaning higher bandwidth cost, leads to smaller reduction, which matches out intuition.

VIII. Related Work

The seminal works [28], [29] propose the idea of GLB to effectively reduce electricity cost of datacenter operators. Later on many works [22], [24], [32], [38] have broadened the landscape of GLB with more practical considerations and design spaces. Instead of studying the benefit of GLB, several works [7], [36] study the impact of GLB on the electricity supply chain and electricity markets. Several works investigate how GLB should be operated in the presence of demand uncertainty and/or market price uncertainty. Both [30] and [39] utilize the long-term forward contracts to reduce operation risk. Similar to our work, [7], [14], [15], [37] deal with uncertainty by bidding in the day-ahead market. However, [14], [15] do not fully exploit the bidding design space, and [7], [37] do not consider demand uncertainty. Instead, our work fully exploits the bidding design space and simultaneously considers the demand and market uncertainty. Note that the problem of designing the optimal bids/offers has also been considered in [2], [3], [13], [23], [27] *etc.*, under various pricing models, but for a single-regional-market scenario. In particular, the authors in [2] design the optimal offer strategies for renewable generation company with given day-ahead market prices but uncertain wind generation.

IX. Concluding Remarks

We develop an algorithm that is proven to minimize the total electricity and bandwidth cost of a CSP in face of workload and price uncertainties, by jointly optimizing strategic bidding in wholesale markets and GLB. Evaluations based on real-world traces show that our algorithm can reduce the CSP's cost by up to 20%. We show that, interestingly, while uncertainty in workloads deteriorates cost saving, uncertainty in day-ahead market prices allows us to achieve a cost reduction even *larger* than the setting without price uncertainty. Our work has several limitations. First, we assume that all the day-ahead market's MCPs and real-time market prices are mutually independent, which may not hold in practice. Second, we assume that the CSP has negligible market power, which may not hold for local markets even though globally datacenters today only consume less than 2% of the total electricity [12]. Finally, we do not model possible strategic behaviours of other market participants. Addressing these limitations is an interesting research direction.

References

[1] "Akamai Internet observatory," available at https://www.akamai.com

[2] E. Y. Bitar, R. Rajagopal, P. P. Khargonekar, K. Poolla, and P. Varaiya, "Bringing wind energy to market," *IEEE Trans. Power Syst.*, vol. 27, no. 3, pp. 1225–1235, 2012.

[3] T. K. Boomsma, N. Juul, and S.-E. Fleten, "Bidding in sequential electricity markets: The Nordic case," *European Journal of Operational Research*, vol. 238, no. 3, pp. 797–809, 2014.
[4] R. Brown, "Report to congress on server and data center energy efficiency: Public law 109-431," *Lawrence Berkeley National Lab*, 2008.
[5] C. Burrus and T. W. Parks, *DFT/FFT and Convolution Algorithms: Theory and Implementation*. John Wiley & Sons, Inc., 1991.
[6] "CAISO archive," available at http://www.caiso.com.
[7] J. Camacho, Y. Zhang, M. Chen, and D. M. Chiu, "Balance your bids before your bits: The economics of geographic load-balancing," in *Proc. ACM e-Energy*, 2014.
[8] A. L. Custódio, H. Rocha, and L. N. Vicente, "Incorporating minimum frobenius norm models in direct search," *Computational Optimization and Applications*, vol. 46, no. 2, pp. 265–278, 2010.
[9] A. L. Custódio and L. N. Vicente, "Using sampling and simplex derivatives in pattern search methods," *SIAM Journal on Optimization*, vol. 18, no. 2, pp. 537–555, 2007.
[10] E. D. Dolan, R. M. Lewis, and V. Torczon, "On the local convergence of pattern search," *SIAM Journal on Optimization*, vol. 14, no. 2, pp. 567–583, 2003.
[11] "ERCOT archive," available at http://www.ercot.com.
[12] "Facts about data centers," available at http://energy.gov.
[13] S.-E. Fleten and E. Pettersen, "Constructing bidding curves for a price-taking retailer in the Norwegian electricity market," *IEEE Trans. Power Syst.*, vol. 20, no. 2, pp. 701–708, 2005.
[14] M. Ghamkhari, H. Mohsenian-Rad, and A. Wierman, "Optimal risk-aware power procurement for data centers in day-ahead and real-time electricity markets," in *Proc. INFOCOM Workshop on SDP*, 2014.
[15] M. Ghamkhari, A. Wierman, and H. Mohsenian-Rad, "Energy portfolio optimization of data centers," *IEEE Trans. Smart Grid*, 2016.
[16] "Google energy wiki," http://en.wikipedia.org/wiki/Google_Energy.
[17] Y. Guo and Y. Fang, "Electricity cost saving strategy in data centers by using energy storage," *IEEE Trans. Parallel Distrib. Syst.*, vol. 24, no. 6, pp. 1149–1160, 2013.
[18] R. Herranz, A. M. San Roque, J. Villar, and F. A. Campos, "Optimal demand-side bidding strategies in electricity spot markets," *IEEE Trans. Power Syst.*, vol. 27, no. 3, pp. 1204–1213, 2012.
[19] M. Khouja, "The single-period (news-vendor) problem: Literature review and suggestions for future research," *Omega*, vol. 27, no. 5, pp. 537–553, 1999.
[20] J. Koomey, "Growth in data center electricity use 2005 to 2010," *A report by Analytical Press, The New York Times*, 2011.
[21] R. M. Lewis and V. Torczon, "Pattern search methods for linearly constrained minimization," *SIAM Journal on Optimization*, vol. 10, no. 3, pp. 917–941, 2000.
[22] M. Lin, Z. Liu, A. Wierman, and L. L. Andrew, "Online algorithms for geographical load balancing," in *Proc. IGCC*, 2012.
[23] G. Liu, Y. Xu, and K. Tomsovic, "Bidding strategy for microgrid in day-ahead market based on hybrid stochastic/robust optimization," *IEEE Trans. Smart Grid*, vol. 7, no. 1, pp. 227–237, 2016.
[24] Z. Liu, M. Lin, A. Wierman, S. H. Low, and L. L. Andrew, "Greening geographical load balancing," in *Proc. ACM SIGMETRICS*, 2011.
[25] B. Neupane, T. B. Pedersen, and B. Thiesson, "Evaluating the value of flexibility in energy regulation markets," in *Proc. ACM e-Energy*, 2015.
[26] "NYISO archive," available at http://www.nyiso.com.
[27] F. Paganini, P. Belzarena, and P. Monzón, "Decision making in forward power markets with supply and demand uncertainty," in *Proc. CISS*, 2014.
[28] A. Qureshi, R. Weber, H. Balakrishnan, J. Guttag, and B. Maggs, "Cutting the electric bill for Internet-scale systems," in *Proc. ACM SIGCOMM*, 2009.
[29] L. Rao, X. Liu, and W. Liu, "Minimizing electricity cost: Optimization of distributed Internet data centers in a multi-electricity-market environment," in *Proc. IEEE INFOCOM*, 2010.
[30] L. Rao, X. Liu, L. Xie, and Z. Pang, "Hedging against uncertainty: A tale of Internet data center operations under smart grid environment," *IEEE Trans. Smart Grid*, vol. 2, no. 3, pp. 555–563, 2011.
[31] S. M. Ross, *Stochastic processes*. Wiley, New York, 1996.
[32] H. Shao, L. Rao, Z. Wang, X. Liu, Z. Wang, and K. Ren, "Optimal load balancing and energy cost management for Internet data centers in deregulated electricity markets," *IEEE Trans. Parallel and Distrib. Syst.*, vol. 25, no. 10, pp. 2659–2669, 2014.
[33] Y. Shi, B. Xu, B. Zhang, and D. Wang, "Leveraging energy storage to optimize data center electricity cost in emerging power markets," in *Proc. ACM E-Energy*, 2016.
[34] J.-S. Song, "The effect of leadtime uncertainty in a simple stochastic inventory model," *Management Science*, vol. 40, no. 5, pp. 603–613, 1994.
[35] Q. Sun, S. Ren, C. Wu, and Z. Li, "An online incentive mechanism for emergency demand response in geo-distributed colocation data centers," in *Proc. ACM e-Energy*, 2016.
[36] P. Wang, L. Rao, X. Liu, and Y. Qi, "D-pro: Dynamic data center operations with demand-responsive electricity prices in smart grid," *IEEE Trans. Smart Grid*, vol. 3, no. 4, pp. 1743–1754, 2012.
[37] P. Wang, Y. Zhang, L. Deng, M. Chen, and X. Liu, "Second chance works out better: Saving more for data center operator in open energy market," in *Proc. CISS*, 2016.
[38] R. Wang, N. Kandasamy, C. Nwankpa, and D. R. Kaeli, "Datacenters as controllable load resources in the electricity market," in *Proc. IEEE ICDCS*, 2013.
[39] L. Yu, T. Jiang, Y. Cao, and Q. Zhang, "Risk-constrained operation for Internet data centers in deregulated electricity markets," *IEEE Trans. Parallel Distrib. Syst.*, vol. 25, no. 5, pp. 1306–1316, 2014.
[40] X.-P. Zhang, *Restructured Electric Power Systems: Analysis of Electricity Markets with Equilibrium Models*. John Wiley & Sons, 2010.
[41] Y. Zhang, L. Deng, M. Chen, and P. Wang, "Joint bidding and geographical load balancing for datacenters: Is uncertainty a blessing or a curse?" *CUHK, Tech. Rep. 2016, https://staff.ie.cuhk.edu.hk/%7Emhchen/papers/BGLBInfocomTech.pdf*.
[42] ——, "Joint bidding and geographical load balancing for datacenters: Is uncertainty a blessing or a curse?" in *Proc. IEEE INFOCOM*, 2017.

Appendix

A. Proof of Theorem 1

Proof: To prove Theorem 1, we firstly provide Proposition 2 and 3 to aid our analysis.

The discussions in Proposition 2 and 3 only involve one datacenter, so we hide the GLB decision $\boldsymbol{\alpha}$ and abuse the notations a little bit to lighten the formula. We will denote $\mathsf{Cost}_j(q(p), f_V(v))$ as the electricity cost of datacenter j when its demand follows $f_V(v)$ and it submits a bidding curve $q(p)$.

***Proposition** 2:* Given two feasible[7] demands $\tilde{V}$ and V with $\tilde{V} = \delta V$, where $\delta \in (0, 1)$ is a constant, we can have

$$\mathsf{Cost}_j(\delta q(p), f_{\tilde{V}}(v)) = \delta \mathsf{Cost}_j(q(p), f_V(v)), \tag{18}$$

for any $q(p) \in \mathcal{Q}$.

***Proposition** 3:* Given two feasible demands V^1 and V^2 with PDF $f_{V^1}(v)$ and $f_{V^2}(v)$, if $q^1(p), q^2(p) \in \hat{\mathcal{Q}}_j$ and $V^1 + V^2$ is also feasible, we can have

$$\begin{aligned}&\mathsf{Cost}_j(q^1(p) + q^2(p), f_{V^1+V^2}(v)) \leq \\ &\mathsf{Cost}_j(q^1(p), f_{V^1}(v)) + \mathsf{Cost}_j(q^2(p), f_{V^2}(v)).\end{aligned} \tag{19}$$

The proofs of Proposition 2 and Proposition 3 involve tedious technical analysis and are deferred in [41].

Now we are ready to prove Theorem 1 by following steps,

To prove **P2** is convex, it is enough to show that its objective function is convex over its feasible region. And we only need to show that $\mathsf{ECost}_j\,(q_j(p), \alpha)$ is convex in $(q_j(p), \alpha)$.

Let $V^1 = (\alpha^1 \mathbf{D})_i$, $V^2 = (\alpha^2 \mathbf{D})_i$ and $\alpha = \delta\alpha^1 + (1-\delta)\alpha^2$, we have $V = (\alpha D)_i = \delta V^1 + (1-\delta)V^2$. If the distributions for V^1 and V^2 are $f^1(y)$ and $f^2(y)$, the distribution for Y is given

[7]Demand V is feasible means that the maximum value of V is less than or equal to the datacenter's capacity.

by $\tilde{f}^1 \odot \tilde{f}^2(y)$, where $\tilde{f}^1(y)$ and $\tilde{f}^2(y)$ are the distributions for δV^1 and $(1-\delta)V^2$. Then,

$$\begin{aligned}
&\delta \mathsf{ECost}_j\left(q_j^1(p), \alpha^1\right) + (1-\delta)\mathsf{ECost}_j\left(q_j^2(p), \alpha^2\right) \\
=&\delta \mathsf{Cost}_j(q^1(p), f^1(v)) + (1-\delta)\mathsf{Cost}_j(q^2(p), f^2(v)), \\
\overset{(E_a)}{=}&\mathsf{Cost}_j(\delta q_j^1(p), \tilde{f}^1(v)) + \mathsf{Cost}_j(q_j^2(p), \tilde{f}^2(v)), \\
\overset{(E_b)}{\geq}&\mathsf{Cost}_j(\delta q^1(p) + (1-\delta)q^2(p), f_{\delta V^1 + (1-\delta)V^2}(v)), \\
=&\mathsf{ECost}_j\left(\delta q_j^1(p) + (1-\delta)q_j^2(p), \delta\alpha^1 + (1-\delta)\alpha^2\right).
\end{aligned}$$

(E_a) and (E_b) are established by Proposition 2 and Proposition 3, respectively.

Moreover, to prove that **P1** and **P2** have the same optimal solution, we only need to show that, with any $\boldsymbol{\alpha}$, the optimal bidding curve of datacenter j belongs to $\hat{\mathcal{Q}}_j$, which is true by Theorem 2.The proof is complete. ■

B. *Proof of Theorem 2*

Proof: To solve $\mathbf{EP}_j(\boldsymbol{\alpha})$, we need to assign a value $q_j(p)$ for each p, to specify how much electricity to buy for any realization of MCP.

The sketch of the proof is as follows: We note that there is a constraint that $q_j(p) \in \hat{\mathcal{Q}}_j$. In the following, we first ignore this constraint and solve the relaxed problem optimally. Then we will show that the optimal solution of the relaxed problem actually satisfies this constraint and thus is optimal to the original problem $\mathbf{EP}_j(\boldsymbol{\alpha})$. We minimize the objective of unconstraint $\mathbf{EP}_j(\boldsymbol{\alpha})$ by minimizing the function value inside the integral for each p.

Now, let $c(q) = pq - \beta p \int_0^q (q-v) f_{V_j}(v)dv + \mu_j^{\mathsf{RT}} \int_q^{\bar{v}_j} (v-q) f_{V_j}(v)dv$, we can have

$$\begin{aligned}
\frac{dc(q)}{dq} &= p - \mu_j^{\mathsf{RT}} \int_q^{\bar{v}_j} f_{V_j}(v)dv - \beta p \int_0^q f_{V_j}(v)dv \\
&= p - \mu_j^{\mathsf{RT}} + (\mu_j^{\mathsf{RT}} - \beta p) \int_0^q f_{V_j}(v)dv.
\end{aligned}$$

We discuss the form of the optimal solution as follows,

- If $p \leq \mu_j^{\mathsf{RT}}$, $\mu_j^{\mathsf{RT}} \geq \beta p$ and $\frac{dc(q)}{dq}$ increases with q. The optimal solution can be obtained by solving $\frac{dc(q)}{dq} = 0$ and the solution is $q_j^*(p) = F_{V_j}^{-1}\left(\frac{\mu_j^{\mathsf{RT}} - p}{\mu_j^{\mathsf{RT}} - \beta p}\right)$.
- If $p \in \left(\mu_j^{\mathsf{RT}}, \mu_j^{\mathsf{RT}}/\beta\right)$, $p - \mu_j^{\mathsf{RT}} \geq 0$ and $\mu_j^{\mathsf{RT}} - \beta p \geq 0$, we have $\frac{dc(q)}{dq} \geq 0$. The optimal solution is $q_j^*(p) = 0$.
- If $p \geq \mu_j^{\mathsf{RT}}/\beta$, $\mu_j^{\mathsf{RT}} - \beta p \leq 0$ and we can observe that $\frac{dc(q)}{dq} \geq p - \mu_j^{\mathsf{RT}} + (\mu_j^{\mathsf{RT}} - \beta p) \geq 0$. Then the optimal solution is $q_j^*(p) = 0$.

The we can get that the optimal solution to the relaxed problem is

$$q_j^*(p;\boldsymbol{\alpha}) = \begin{cases} F_{V_j}^{-1}\left(\frac{\mu_j^{\mathsf{RT}} - p}{\mu_j^{\mathsf{RT}} - \beta p}\right), & \text{if } p \in \left[0, \mu_j^{\mathsf{RT}}\right); \\ 0, \text{otherwise}. \end{cases}$$

Note that $\frac{\mu_j^{\mathsf{RT}} - p}{\mu_j^{\mathsf{RT}} - \beta p} \in (0,1)$ decreases with p and $F_{V_j}^{-1}(\cdot)$ is an increasing function, so $q_j^*(p;\boldsymbol{\alpha}) \in \hat{\mathcal{Q}}_j$. Also, in the processing of obtaining $q_j^*(p;\boldsymbol{\alpha})$, we do not restrict our attention to $\hat{\mathcal{Q}}_j$, instead we search the entire bidding curve design space $\mathcal{Q}$, which meas that $q_j^*(p;\boldsymbol{\alpha})$ is also the optimal bidding curve for **P1**. The proof is complete. ■

C. *Proof of Theorem 4*

Proof: We first describe the complexity to solve our inner-loop problem $\mathbf{EP}_j(\boldsymbol{\alpha})$, *i.e.*, compute the optimal datacenter j's bidding curve $q_j^*(p;\boldsymbol{\alpha})$ through (15) when the GLB decision is given by $\boldsymbol{\alpha}$. We need five steps to obtain $q_j^*(p;\boldsymbol{\alpha})$. (i) We obtain the PDF of U_{ij}, *i.e.*, $f_{U_{ij}}(v)$, for all $i \in [1,N]$. Through (8), we can obtain $f_{U_{ij}}(v)$ in $O(m)$ for each i, and thus get all $f_{U_{ij}}(u)$'s ($\forall i \in [1,N]$) in $O(Nm)$. (ii) We obtain the PDF of datacenter j's allocated demand V_i, *i.e.*, $f_{V_j}(v)$. We can obtain $f_{V_j}(v)$ through (7) by doing convolution $N-1$ times in $O(N^2 m \log(Nm))$ [5]. Note that $f_{V_j}(v)$ could take values at Nm different points. (iii) We obtain the CDF of V_j, *i.e.*, $F_{V_j}(v)$. We can iteratively do summation to obtain $F_{V_j}(v)$ in $O(Nm)$. (iv) We obtain the inverse function of the CDF of V_j, *i.e.*, $F_{V_j}^{-1}(v)$. We only need to inverse all Nm points of $F_{V_j}(v)$, which requires $O(Nm)$ complexity. (v) We obtain the optimal bidding curve $q_j^*(p;\boldsymbol{\alpha})$. Since we have sampled $f_{P_j}(p)$ into a length-m sequence, we only need to get $q_j^*(p;\boldsymbol{\alpha})$ for at most m different values for p. Thus we can construct $q_j^*(p;\boldsymbol{\alpha})$ in $O(m)$ steps. Therefore, the total complexity is the sum of (i)-(v), *i.e.*, $O(Nm) + O(N^2 m \log(Nm)) + O(Nm) + O(Nm) + O(Nm) + O(m) = O(N^2 m \log(Nm))$.

We then analyze the computation complexity of the subroutine $\mathbf{P3\text{-}OBJ}(\boldsymbol{\alpha})$, *i.e.*, evaluating the objective value of **P3** for any given GLB decision $\boldsymbol{\alpha}$. Step 13 needs $O(N^2)$ from (9). Steps 15 is the complexity to compute $q_j^*(p;\boldsymbol{\alpha})$, which requires $O(N^2 m \log(Nm)$. Step 16 is the complexity to compute $\mathsf{ECost}_j\left(q_j^*(p;\boldsymbol{\alpha}), \boldsymbol{\alpha}\right)$ by (12). For any $P_j = p$, the day-ahead trading cost part can be computed in $O(1)$; the rebate of over-supply can be computed in $O(Nm)$; the cost of under-supply can be computed in $O(Nm)$; thus the total complexity for given $P_j = p$ is $O(Nm)$. Since we have sampled $f_{P_j}(p)$ into a length-m sequence, the total complexity to compute $\mathsf{ECost}_j\left(q_j^*(p;\boldsymbol{\alpha}), \boldsymbol{\alpha}\right)$ will be $O(Nm^2)$. Since $\mathbf{P3\text{-}OBJ}(\boldsymbol{\alpha})$ should do N iterations for all datacenters, the total complexity to evaluate $\mathbf{P3\text{-}OBJ}(\boldsymbol{\alpha})$ is $O(N^2 + N(N^2 m \log(Nm) + Nm^2)) = O(N^3 m \log(Nm) + N^2 m^2)$.

Finally we come to analyze the computational complexity of our global solution, *i.e.*, Algorithm 1. During the **while** loop, each iteration requires at most $(2N+1)$ invokes for the subroutine $\mathbf{P3\text{-}OBJ}(\boldsymbol{\alpha})$, and thus incurs $O((2N+1) \times (N^3 m \log(Nm) + N^2 m^2)) = O((N^4 m \log(Nm) + N^3 m^2))$. Suppose that our Algorithm 1 converges in n_{iter} iterations. Then the computational complexity of our Algorithm 1 is $O(n_{\mathsf{iter}}((N^4 m \log(Nm) + N^3 m^2)))$. ■

D. *Proof of Lemma 1*

Proof: To aid our analysis, we introduce two stochastic orderings called "increasing convex ordering" ($\geq_{\text{ic}}$) and "variability ordering" ($\geq_{\text{var}}$), the definitions of which are presented below. And an important property is presented in Proposition 4.

Definition 1: ([34, Definition 4.1]) For two random variables X and Y, $X \geq_{\text{ic}} Y$ if and only if $\mathbb{E}[f(X)] \geq \mathbb{E}[f(Y)]$ for **all** nondecreasing convex functions f.

Definition 2: ([34, Definition 4.8]) Consider two random variables X and Y with the same mean $\mathbb{E}[X] = \mathbb{E}[Y]$, having distribution functions f and g. Suppose X and Y are either both continuous or discrete. We say X is more variable than Y, denoted as $X \geq_{\text{var}} Y$, if the sign of $f - g$ changes exactly twice with sign sequence $+, -, +$.

Proposition 4: ([34, Lemma 4.9]) $X \geq_{\text{var}} Y$ implies that $X \geq_{\text{ic}} Y$.

We consider two electricity demands V_1 and V_2 with the same expectations and V_1 has a larger variance. According to the definition of "variability ordering" and the properties of involved unimodal distributions, $V_1 \geq_{var} V_2$. We denote C_1 and C_2 as the cost of V_1 and V_2 by the optimal bidding curve in (15). Our purpose is to show that $C_1 \geq C_2$.

Let $C_1(p)$ and $C_2(p)$ be the cost expectation conditioning on that the day-ahead MCP is realized as p, and $C_1 = \int_0^{+\infty} C_1(p) f_{P_i}(p)dp$, $C_2 = \int_0^{+\infty} C_2(p) f_{P_i}(p)dp$. It would be sufficient if we can show that $C_1(p) \geq C_2(p), \forall p$.

Also, note that when the day-ahead MCP is fixed as p, the problem $\mathbf{EP}_j(\boldsymbol{\alpha})$ will reduce to the classic Newsvendor problem and (15) is the corresponding optimal solution. According to Proposition 4, we can have $V_1 \geq_{\text{ic}} V_2$. By the following proposition, we can immediately have $C_1(p) \geq C_2(p), \forall p$.

Proposition 5: [34, Proposition 4.3] For the Newsvendor problem, given two future demands D_1, D_2, if $D_1 \geq_{ic} D_2$, $\mathbb{E}[D_1] = \mathbb{E}[D_2]$, then the optimal cost of D_1 is not less than that of D_2.

The proof is complete. ■

E. Proof of Lemma 2

Proof: We first define $C_{\text{opt}}(p)$ as the expected cost *under the optimal bidding strategy* when the day-ahead MCP is realized as p. And the total cost expectation by (15) can be expressed as $\mathbb{E}_P[C_{\text{opt}}(p)]$, where the expectation is taken with respected to the distribution of day-ahead MCP. We consider two stochastic day-ahead MCP denoted by P^1 and P^2 with $\mathbb{E}[P^1] = \mathbb{E}[P^2]$ and P^1 having a larger variance. According to the definition of "variability ordering" and the properties of involved unimodal distributions, $P^1 \geq_{\text{var}} P^2$. Our goal is to show that $\mathbb{E}_{P^1}[C_{\text{opt}}(p)] \leq \mathbb{E}_{P^2}[C_{\text{opt}}(p)]$.

Since $P^1 \geq_{\text{var}} P^2$ implies $P^1 \geq_{\text{ic}} P^2$ (by Proposition 4), according to the following lemma, it will be sufficient to show that $C_{\text{opt}}(p)$ is a **concave** function of p. (A more direct result is that $\mathbb{E}_{P^1}[-C_{\text{opt}}(p)] \geq \mathbb{E}_{P^2}[-C_{\text{opt}}(p)]$ if $-C_{\text{opt}}(p)$ is convex.)

Lemma 4: ([31]) If X and Y are nonnegative random variables with $\mathbb{E}[X] = \mathbb{E}[Y]$, then $X \geq_{\text{ic}} Y$ if and only if $\mathbb{E}[f(X)] \geq \mathbb{E}[f(Y)]$ for all convex functions f.

Let $\alpha \in (0, 1)$ and $p^0 = \alpha p^1 + (1 - \alpha)p^2$. We will show that $C_{\text{opt}}(p^0) \geq \alpha C_{\text{opt}}(p^1) + (1 - \alpha)C_{\text{opt}}(p^2)$.

Recall that $C_{\text{opt}}(p) = pq_j^*(p) - \beta p \int_0^{q_j^*(p)} (q_j^*(p) - v) f_{V_j}(v)dv + \mu_j^{\mathsf{RT}} \int_{q_j^*(p)}^{\bar{v}_j} (v - q_j^*(p)) f_{V_j}(v)dv$. To lighten the formula, we further denote $Q_{\text{over}}(q_j^*(p)) = \int_0^{q_j^*(p)} (q_j^*(p) - v) f_{V_j}(v)dv$ and $Q_{\text{under}}(q_j^*(p)) = \int_{q_j^*(p)}^{\bar{v}_j} (v - q_j^*(p)) f_{V_j}(v)dv$ as the expected over-supply and under-supply, respectively. Then our proof will proceed as follows,

$$
\begin{aligned}
& C_{\text{opt}}(p^0) \\
=& p^0 q_j^*(p^0) - \beta p^0 Q_{\text{over}}(q_j^*(p^0)) + \mu_j^{\mathsf{RT}} Q_{\text{under}}(q_j^*(p^0)) \\
\overset{(E_a)}{=}& \alpha \left(p^1 q_j^*(p^0) - \beta p^1 Q_{\text{over}}(q_j^*(p^0)) + \mu_j^{\mathsf{RT}} Q_{\text{under}}(q_j^*(p^0)) \right) + \\
& (1-\alpha) \left(p^2 q_j^*(p^0) - \beta p^2 Q_{\text{over}}(q_j^*(p^0)) + \mu_j^{\mathsf{RT}} Q_{\text{under}}(q_j^*(p^0)) \right) \\
\overset{(E_b)}{\geq}& \alpha \left(p^1 q_j^*(p^1) - \beta p^1 Q_{\text{over}}(q_j^*(p^1)) + \mu_j^{\mathsf{RT}} Q_{\text{under}}(q_j^*(p^1)) \right) + \\
& (1-\alpha) \left(p^2 q_j^*(p^2) - \beta p^2 Q_{\text{over}}(q_j^*(p^2)) + \mu_j^{\mathsf{RT}} Q_{\text{under}}(q_j^*(p^2)) \right) \\
=& \alpha C_{\text{opt}}(p^1) + (1-\alpha) C_{\text{opt}}(p^2).
\end{aligned}
$$

We get step (E_a) by replacing the p^0 outside $q_j^*(\cdot)$ with $\alpha p^1 + (1 - \alpha)p^2$ and rearranging the terms. And (E_b) is due to the fact that $q_j^*(p^1)$ and $q_j^*(p^2)$ are the optimal electricity procurement. (remember that we obtain $q_j^*(p^1), q_j^*(p^2)$ by minimizing $pq_j^*(p) - \beta p Q_{\text{over}}(q_j^*(p)) + \mu_j^{\mathsf{RT}} Q_{\text{under}}(q_j^*(p))$ for p^1, p^2). The proof is completed. ■

F. Proof of Lemma 3

Proof: We firstly reformulate the cost function from (12) to the following one,

$$
\begin{aligned}
& \mathsf{ECost}_j(q(p)) \\
=& \int_0^{+\infty} f_P(p) \left[(\mu_j^{\mathsf{RT}} - \beta p) \int_0^{q(p)} (q(p) - v) f_V(v)dv - (\mu_j^{\mathsf{RT}} - p) q(p) \right] dp \\
& \quad + \mu_j^{\mathsf{RT}} \mathbb{E}[V] \\
\overset{(E_a)}{=}& \int_0^{\mu_j^{\mathsf{RT}}} f_P(p) \left[(\mu_j^{\mathsf{RT}} - \beta p) \int_0^{q(p)} F_V(v)dv - (\mu_j^{\mathsf{RT}} - p) q(p) \right] dp \\
& \quad + \mu_j^{\mathsf{RT}} \mathbb{E}[V].
\end{aligned}
$$

(E_a) comes from the facts that $q(p) = 0$ for $p \geq \mu_j^{\mathsf{RT}}$ and

$$
\begin{aligned}
& \int_0^{q(p)} (q(p) - v) f_V(v)dv = \int_0^{q(p)} (q(p) - v) dF_V(v) \\
=& (q(p) - v) F_V(v)|_0^{q(p)} - \int_0^{q(p)} F_V(v) d(q(p) - v) \\
=& \int_0^{q(p)} F_V(v)dv.
\end{aligned}
$$

We will prove the inequality in the following steps.

$$
\begin{aligned}
& |\mathsf{ECost}_j(q^1(p)) - \mathsf{ECost}_j(q^2(p))|^2 \\
=& |\int_0^{\mu_j^{\mathsf{RT}}} f_P(p) \left[(\mu_j^{\mathsf{RT}} - \beta p) \int_{q^2(p)}^{q^1(p)} F_V(v)dv - (\mu_j^{\mathsf{RT}} - p)(q^1(p) - q^2(p)) \right] dp|^2 \\
\overset{(E_b)}{\leq}& |\int_0^{\mu_j^{\mathsf{RT}}} f_P(p) \left[(\mu_j^{\mathsf{RT}} - \beta p) |\int_{q^2(p)}^{q^1(p)} F_V(v)dv| + (\mu_j^{\mathsf{RT}} - p)|q^1(p) - q^2(p)| \right] dp|^2 \\
\overset{(E_c)}{\leq}& |\int_0^{\mu_j^{\mathsf{RT}}} f_P(p) \left[(\mu_j^{\mathsf{RT}} - \beta p)|q^1(p) - q^2(p)| + (\mu_j^{\mathsf{RT}} - p)|q^1(p) - q^2(p)| \right] dp|^2 \\
=& |\int_0^{\mu_j^{\mathsf{RT}}} f_P(p) \left[(2\mu_j^{\mathsf{RT}} - \beta p - p)|q^1(p) - q^2(p)| \right] dp|^2 \\
\overset{(E_d)}{\leq}& \int_0^{\mu_j^{\mathsf{RT}}} \left[f_P(p)(2\mu_j^{\mathsf{RT}} - \beta p - p) \right]^2 dp \int_0^{\mu_j^{\mathsf{RT}}} |q^1(p) - q^2(p)|^2 dp.
\end{aligned}
$$

Step (E_b) is obtained by replacing the two terms in the integral by their absolute values, which is similar to $|a + b| \leq ||a| + |b||$. Step (E_c) is due to the fact that $F(v) \leq 1$ and (E_d) is the application of Cauchy-Schwarz inequality. ■